Activation of the mechanistic target of rapamycin complex 1 (mTORC1) in thyrocytes induces follicular hyperplasia and impaired thyroid hormone synthesis

Camila Rossetti[1], Bruna Lourençoni[1,2], Flavia Peçanha[1], Vania Nosé[3], John Lew[4], Everardo Carneiro[2], Ernesto Bernal-Mizrachi[1,5] and Joao Pedro Werneck-de Castro[1]

[1] Division of Endocrinology, Diabetes and Metabolism, University of Miami, Miami, FL, USA
[2] Obesity and Comorbidities Research center (OCRC), Department of Structural and Functional Biology, Institute of Biology, University of Campinas, Campinas, SP, Brazil
[3] Massachusetts General Hospital, Harvard University, Boston, MA, USA
[4] Department of Surgery, University of Miami, Miami, FL, USA
[5] Miami VA Health Care System, Miami, FL, USA

ABSTRACT

The serine-threonine protein kinase mechanistic target of rapamycin complex 1 (mTORC1) plays a pivotal role in regulating cellular metabolism, growth, and proliferation. The thyroid gland is a frequent site of abnormal epithelial cell growth and proliferation that can lead to thyroid dysfunction. In the thyroid gland, the PI3K-Akt-mTOR pathway is abnormally overactive in tumors and has been linked to increased aggressiveness in thyroid cancer. However, our understanding of mTORC1's role in thyrocytes is primarily based on *in vitro* studies, leaving its *in vivo* function unclear. To bridge this knowledge gap, we developed a novel mouse model of mTOR gain of function specifically in thyrocytes by crossing the mouse with thyroperoxidase (TPO)-driven cre recombinase expression with the Tuberous Sclerosis Complex 2 (TSC2)-floxed mouse. TSC2 acts as an intracellular inhibitor of mTORC1 and its conditional disruption leads to overactivation of mTOR activity. In TPO-TSC2^{KO} mice, thyroid glands exhibited 70-80% less TSC2 protein and mRNA levels. Concomitantly, the TSC2 knockout in thyrocytes led to increased protein expression of mTORC1 target pS6 and decreased expression of mTORC2 target Akt phosphorylated in serine 473. Thyroid gland size was bigger in the TPO-TSC2^{KO} mice as early as 1-month of age and continued to grow throughout life in both genders. Microscopic examination revealed significant heterogeneity among thyroid follicles in the TPO-TSC2^{KO} mice, and their thyroids present larger follicles, colloid and epithelium. Overactivation of mTORC1 resulted in increased thyrocyte proliferation, as indicated by Ki67 staining, and elevated Cyclin D3 levels. Chronic mTOR overactivation suppressed mRNA expression of key genes involved in thyroid hormone biosynthesis such as thyroglobulin, thyroperoxidase and sodium-iodide symporter in both male and female mice. As a result, TPO-TSC2^{KO} mice exhibited slight hypothyroidism with 20% less plasma thyroxine and 2-fold increase in TSH levels. Systemic treatment with rapamycin, an mTORC1 inhibitor, prevented thyroid mass expansion and gene expression alterations in TPO-TSC2^{KO} mice. Finally, TPO-TSC2^{KO} mice aged 12 months or older developed aberrant thyroid conditions including follicular hyperplasia, inflammation and thyroid tumors. In summary, our study demonstrates that mTORC1 gain of function specifically in thyrocytes leads to alterations in follicle morphology and impairs thyroid gland function.

INTRODUCTION

The thyroid gland is often the site of abnormal growth and proliferation of epithelial cells, which can result in thyroid dysfunction [1-4]. The exact mechanisms that lead to these abnormalities in the thyroid gland are not fully understood. However, it is suggested that elevated levels of circulating insulin/IGF1 and TSH may play a role in the pathogenesis [1, 5].

TSH, or thyrotrophin, is a key regulator of thyroid function [6]. The effects of TSH are primarily mediated through activation of adenylate cyclase by the a-subunit of stimulatory GTP-binding protein (Gsa)[7]. In addition to this, TSH can also activate the Gq/phospholipase C cascade [8]. TSH has a positive regulatory effect on almost all the steps of hormone production and secretion [9]. Specifically, TSH stimulates the expression of several key components involved in thyroid hormone production: the sodium iodide symporter (NIS), thyroperoxidase (TPO), thyroglobulin (Tg), and it aids in the generation of H_2O_2. It also increases the formation of T_3 relative to T_4, alters the priority of iodination and hormonogenesis among tyrosyls, and promotes the rapid internalization of Tg by thyrocytes [10]. TSH is also responsible for promoting thyrocyte proliferation, growth, and vasculature function [9]. In thyrocytes, phosphatidyl-inositol-3-kinase (PI3K) pathway plays a pivotal role in controlling both cell proliferation and differentiation. Activation of TSH receptor can lead to PI3K activation [11, 12]. Additionally, this pathway can be activated in thyrocytes by various growth factors such as insulin/insulin like growth factor 1 (IGF1), hepatocyte growth factor, or epidermal growth factor [13]. The immediate downstream effector of PI3K signaling is Akt [14]. Activated Akt has many substrates within the cell, such as TSC2 and PRAS40, leading to the activation of mechanistic target of rapamycin (mTOR) [15].

The serine–threonine protein kinase mTOR plays a crucial role in regulating cellular metabolism, growth, and proliferation [16]. mTOR operates within two distinct multi-protein complexes: mTOR complex 1 (mTORC1) and mTORC complex 2 (mTORC2). mTORC1 acts as a downstream effector for growth factors, energy and nutrients, particularly amino acids. The regulation of the mTORC1 pathway is achieved through the convergence of these signals on the tuberous sclerosis complex (TSC1/2). TSC1/2 complex functions as a GTPase-activating protein for Rheb, catalyzing the conversion from the active Rheb-GTP state to the inactive GDP-bound state. mTOR can only transition into a catalytic position after the complex binds to active Rheb-GTP and this implies that TSC1/2 acts as a critical 'molecular brake' for mTORC1 activation [17]. mTORC1 tightly regulates protein synthesis by phosphorylating the eukaryotic initiation factor 4E-binding proteins (4E-BPs) and p70S6 kinase 1 (S6K). While phosphorylation of 4E-BP1 enhances 5' cap-dependent translation of mRNA [18, 19], activation of S6K promotes ribosomal synthesis and boosts the rate of translation elongation [20, 21]. By regulating all necessary cellular metabolic pathways, mTORC1 is essential for cell growth and supports proliferation.

Research suggests that IGF1 works in synergy with TSH to promote thyrocyte proliferation [13, 22, 23]. When IGF1 receptor is genetically disrupted in mice, it impairs the mTORC1 activation induced by goiter (high TSH levels) and hinders thyroid expansion [24]. This suggests that the absence of mTORC1 activation by IGF1 (and Insulin) mediates goiter responses. In contrast, it has been reported that IGF1 receptor knockout mice [25] and mice with double knockout for IGF1 and Insulin receptors [26] exhibit intense mTORC1 activation, proliferation, and growth in thyrocytes. This indicates that TSH-mediated mTORC1 activation compensates for the lack of Insulin/IGF-1 signaling through PI3K-Akt-mTORC1 pathway. Importantly, mTORC1 inhibition by systemic treatment with rapamycin diminished thyrocyte proliferation in response to goitrogenic conditions [27]. These studies collectively demonstrate that mTORC1 is activated by IGF1 and TSH *in vivo*, suggesting a potential role for mTORC1 in thyrocyte proliferation and growth. Importantly, dysregulation of mTORC1, as observed in many types of cancer, is a characteristic feature of thyroid cancer. There is increasing evidence that the mTORC1 pathway plays a role in the progression of more lethal forms of thyroid cancer [28-33]. Furthermore, mTORC1 is activated in aggressive forms of papillary [30, 34] and anaplastic thyroid cancers [35-39].

While the PI3K-Akt-mTOR pathway is clearly involved in thyrocyte proliferation, its role in thyroid hormone synthesis and function remains a topic of debate [40-42]. Studies have shown that IGF-1 inhibits the *NIS* expression in rat FRTL-5 and PCCL3 thyrocytes [12, 15, 43]. This inhibitory effect has been demonstrated to be mediated by PI3K [12, 15, 43] or mTORC1 [15] *in vitro*. Contrastingly, recent studies have shown that TSH and IGF-1 elicited additive effects on TPO, Tg and the type-1 deiodinase (Dio1) expression, and synergistic effects on *NIS* mRNA and protein in primary human thyrocytes [41, 42]. The discrepancy between these findings is likely due to the *in vitro* conditions, as TSH fully induces NIS expression only when thyrocytes are organized as follicles [44]. Importantly, the *in vitro* setting does not allow for the investigation of hormone secretion and synthesis because the gland loses its crucial angiofollicular unit and cell polarity [9]. The role of mTOR in thyroid function is clinically relevant. Patients suffering from Tuberous Sclerosis, which involves overactivation of mTORC1 due to mutations in the TSC1/2 genes, often present with thyroid abnormalities [45-51]. Furthermore, whether mTORC1 controls NIS expression

is clinically significant because the loss of NIS expression in thyroid cancer is proposed as the mechanism for refractory response to radioiodine therapy [35].

The potential consequences of mTORC1 dysregulation in thyroid physiology have been largely understudied, with previous investigations primarily focused on thyroid cancer pathogenesis. Furthermore, our current understanding of mTORC1`s role in thyrocytes is predominantly based on *in vitro* studies, which fail to fully recapitulate *in vivo* thyroid hormone synthesis and secretion due to the disruption of the critical angio-follicular unit and cell polarity. As a result, there is a pressing need to evaluate the *in vivo* impact of mTORC1 on thyrocyte function and growth. To gain a better understanding of mTOR`s role in thyroid, we generated a mouse model of mTORC1 gain of function by deleting TSC2 gene in thyrocytes (TPO-TSC2^{KO} mice). The overactivation of mTORC1 led to an enlarged thyroid with larger follicles and a higher proliferation rate. Importantly, these knockout mice present decreased expression of genes crucial for thyroid hormone biosynthesis (NIS, TPO and TG) and reduced thyroxine levels, while TSH levels increased. The inhibition of mTORC1 in TPO-TSC2^{KO} mice with rapamycin effectively blocked the expansion of thyroid mass and the alterations in gene expression. Finally, TPO-TSC2^{KO} mice aged 12 months or older presented thyroid tumors. Collectively, this data establishes mTORC1 as a crucial intracellular component implicated in the biosynthesis of thyroid hormones.

MATERIAL AND METHODS

Animals

All experimental procedures were planned following the American Thyroid Association guide to investigating thyroid hormone economy and action in rodent and cell models [52] and approved by the local Institutional Animal Care and Use Committee (IACUC 20-166). All mice were maintained at 22 ± 1 °C on a 12h light–dark cycle, with free access to food and water. Thyroid-specific *TSC2* knockout mice (TPO-TSC2^{KO}) were generated by crossing *Tsc2$^{flox/flox}$* mice with mice expressing the Cre recombinase gene under the control of the thyroid peroxidase (TPO) promoter. The *Tsc2$^{flox/flox}$* mice harbor a modified endogenous *TSC2* gene with *loxP* sites flanking exons 2 to 4 [53]; Fig 1A). TPO-driven cre recombinase mouse was kindly donated by Dr. Shioko Kimura from the National Cancer Institute/National Institutes of Health [54]. The experiments were performed on male and female mice that were on a mixed 129 x C57BL/6 background. We used littermates *Tsc2$^{flox/flox}$* mice as controls. Rapamycin-treated mice received daily intraperitoneal injections of either 2 mg/Kg of b.w. Rapa (Cayman Chemical Company, Ann Harbor, MI) or vehicle (5.2% Poly(ethylene glycol) and 5.2% Tween 80; Sigma-Aldrich, St. Louis, MO) from weaning (3 weeks of age) to 2 months of age (Fig 6).

Body composition and hormone measurements

Body weight and glycemia were followed monthly from weaning to 12 months of age. Dual-energy X-ray absorptiometry (DEXA; Lunar Pixi, Janesville, WI) determined lean body mass and fat mass. Mice were fasted for 4-5 hours and anesthetized with ketamine-xylazine (36 mg/kg and 4 mg/kg) before imaging. Blood samples were collected in K_2EDTA-coated tubes and centrifuged at 1,000 x g for 10 minutes within 30 minutes of collection. Total Thyroxine (T_4) and total Triiodothyronine (T_3) were measured using 25 µL of plasma and ELISA kits from Cusabio (Houston, TX). TSH levels were determined using Luminex multiplex technologies with one-plex beads (Milliplex Mouse Pituitary Magnetic Bead Panel, Millipore, Burlington, MA). All hormone determinations were performed according to the manufacturer`s instructions.

Western blotting

One thyroid lobe per animal was lysed in a buffer containing 125 mM Tris (pH 6.8), 1 mM dithiothreitol, 2% SDS, 1 µM phenylmethylsulfonyl fluoride, and protease and phosphatase inhibitor cocktails (Roche Diagnostics, Indianapolis, IN). Protein quantity was measured using the bicinchoninic acid (BCA) assay method and 30 µg of protein were separated by electrophoresis into 4-20% gradient SDS–PAGE gels. Then, proteins were transferred to polyvinylidene difluoride (PVDF) membranes (Millipore, Burlington, MA) overnight. After blocking for 1 h in blocking buffer, membranes were incubated overnight at 4 °C with primary antibodies listed in Table 1. Immunocomplexes were detected using fluorescent secondary antibodies and the Odissey FC Imager (LI-COR Biosciences, Lincoln, NE). Bands were submitted to densitometric analysis by ImageJ 1.43u software and normalized to tubulin, β-actin or total S6 (tS6). Images were cropped for presentation.

TABLE 1. Antibodies used for Western-blot

Antibody	Specie	Source	Catalog	Concentration
p-Akt Ser^{473}	Rabbit	Cell Signaling	#4060	1:1000
β-Actin	Mouse	Sigma-Aldrich	#A5441	1:5000
Cyclin D2	Rabbit	Cell Signaling	#3741S	1:1000
Cyclin D3	Mouse	Cell Signaling	#2936S	1:1000
NIS	Rabbit	Millipore	#ABC1453	1:1000
p-S6 $Ser^{240-244}$	Rabbit	Cell Signaling	#5364	1:5000
Total S6	Mouse	Cell Signaling	#2317S	1:750
Tuberin/TSC2	Rabbit	Cell Signaling	#4308	1:1000
Tubulin	Mouse	Sigma-Aldrich	#T5168	1:5000

Real-time PCR

One thyroid lobe was used for total RNA extraction according to the manufacturer's protocol (RNeasy Micro Kit, Qiagen, Hilden, Germany). RNA concentration and purity were determined by spectrophotometry (ratio 260/280 nm). cDNA was synthesized using a reverse transcriptase reaction (High-Capacity cDNA Reverse Transcription kit, Applied Biosystems, Waltham, MA). Real-time PCRs were run in duplicate using PerfeCTa SYBR Green FastMix ROX gene expression assay (Quantabio, Beverly, MA) in a QuantStudio 3 real-time PCR system (Applied Biosystems, Waltham, MA). mRNA expression was calculated using the relative standard curve method and normalized for the housekeeping gene *18S* or *CycloB.* Primers were validated using a standard curve prepared with a mixture of cDNA from all samples ($r^2 > 0.98$ and efficiency ~80-110%) and are listed in Table 2.

TABLE 2. Primer sequences for gene amplification via RT-qPCR

Gene name	Amplification length (bp)	Reference sequence	Sequence
Dio1	111	NM_007860.4	F: CAGAGACTGGAAGACAGGGC R: GGGCCTGCTGCCTTGAAT
Mct8	150	NM_011040.4	F: GCTTCGGCTGGATAGTGGTG R: CTCCGACCCATGCTGCTT
Nis	138	NM_053248	F: CCAGTACCTAGAACTGCGCTT R: ATGTCCAACCCGGTCACTTG
Pax8	200	NM_011040.4	F: ACTCGATCAGATCCGGCCAT R: GCTGCCAGTCTCGTAGTACC
Tg	182	NM_009375.2	F: CCTGTCCAGGAAAGTGGGTC R: GTGGACACTGTGGGCTTTCA
Tpo	136	NM_009417.3	F: GATAGTAATTTGCAGGTGGACACA R: CTCTATTCGCACAGGAGGACC
Tsc2	179	NM_011647.3	F: TCTCTAGTACTGCCCTGCCC R:GCATTCACCACTCAGTTCTCTC
Tshr	199	NM_011648.5	F: ACAAAGCTGGATGCTGTTTACC R: ACAGCGGGAGCTTTTTGAGA
Ttf-1	134	NM_009442.2	F: CATTGTCGCTGGGGACAGG R: TCTCCAAGCACTGAGAGGGA

Histological analysis

Thyroids were collected and fixed in 4% paraformaldehyde overnight, followed by dehydration in ethanol. Tissues were embedded in paraffin and 5 µm sections were stained with Periodic Acid-Schiff (PAS) and Hematoxylin and Eosin for morphometric analysis, according to [52, 55, 56]. High-resolution images were obtained using a digital camera (DFC360FX camera, Leica Microsystems, Wetzlar, Germany) coupled to a microscope (Leica DM5500B, Leica Microsystems). High-quality images were captured with Leica Application Suite X (LAS X). PAS images were used for the quantification of follicular, colloid, and epithelium (total area - colloid) areas. At least 100 follicles per mouse were included in the analysis. Images were captured using a digital camera connected to a microscope [52, 55, 56]. All the measurements were performed using the ImageJ software.

Thyrocyte proliferation quantification

Mouse thyroids attached to the trachea were fixed by immersion in 4% paraformaldehyde overnight at 4°. They were then cryoprotected in 70% ethanol at 4°C and embedded in paraffin. To determine the number of proliferating thyrocytes, 5 µm sections were stained for Ki-67 and TTF-1 (nuclear thyroid marker) using anti-Mo/Rt Ki-67 (Invitrogen, Waltham, MA)

and anti-TTF-1 (D2E8) Rabbit mAb (Cell Signaling Technology, Danvers, MA) primary antibodies. Fluorescent images were captured with a Leica DM5500B microscope equipped with a motorized stage and a DFC360FX camera (Leica Microsystems, Wetzlar, Germany). The microscope was controlled by the OASIS-blue PCI controller and the Leica Application Suite X (LAS X). Ki-67^{+} and TFF-1^{+} cells were quantified by ImageJ.

Statistical analysis

Results are presented as mean ± standard error of the mean (SEM). Data were first analyzed using the Shapiro-Wilk normality test. If normally distributed, data were analyzed using: 1) Student`s unpaired t-test for comparisons between 2 groups; 2) *one-way* ANOVA for comparisons between more than 2 groups; or 3) *two-way* ANOVA to analyze the effect of two independent factors. All ANOVA tests were followed by Tukey post-hoc analysis. If data were not normally distributed, the Mann-Whitney U test was used. Results were considered statistically significant if $p < 0.05$. Statistical analyses and graphing were performed using GraphPad Prism version 9.4 (GraphPad Software, San Diego, CA, US).

RESULTS

Activation of mtorc1 in thyrocytes promotes thyroid gland growth

To investigate the role of mTORC1 pathway in thyrocytes, we generated a new mouse model of mTORC1 gain of function specifically in thyrocytes by crossing a TSC2-floxed mouse with a mouse with thyroid peroxidase (TPO)-driven cre recombinase expression (TPO-TSC2^{KO} mice; Fig 1A). Thyroids of TPO-TSC2^{KO} mice had a 70-80% decrease in TSC2 protein levels and a 6-fold induction of mTORC1 activity (pS6) in both females and males (Fig 1). In contrast, mTORC2 activity decreased in the TPO-TSC2^{KO} mice thyroids (lower pAkt Ser^{473} phosphorylation). Male and female TPO-TSC2^{KO} mice did not gain weight as littermate control mice and had less fat mass at 12 months of age (Fig 2 A-C). mTORC1 overactivation promoted a remarkable thyroid gland enlargement as early as 1 month of age (Fig 2D). Thyroid mass was higher in TSC2 knockout mice compared to the thyroid of control animals at 1, 2, 6 and 12 months of age (Fig 2D-F).

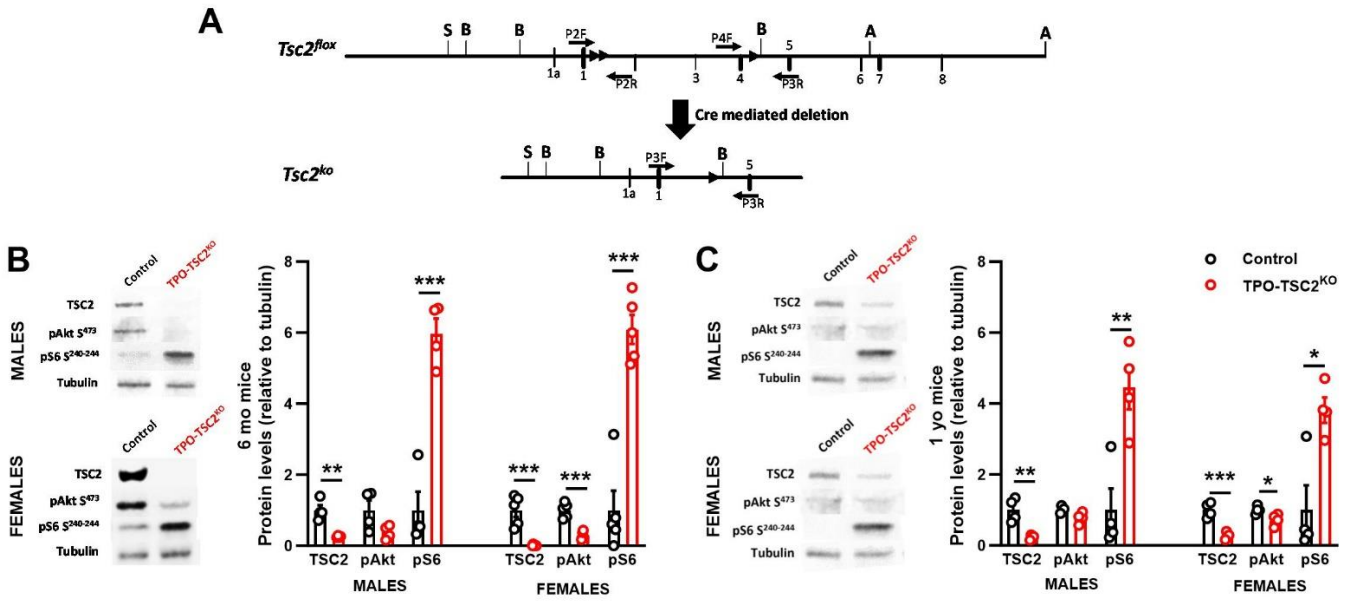

Figure 1. Validation of the TPO-TSC2 knockout model. (a) Gene-targeting construct. Exons are indicated by black boxes labeled with exon numbers. LoxP sites are marked by black triangles. The loxP-frt-neo-frt cassette was inserted in intron 1 and a loxP-BamHI site in intron 4. (b) Thyroid TSC2, pAkt Ser^{473} and pS6 Ser$^{240-244}$ protein expression in 6 months old males and females. (c) Thyroid TSC2, pAkt Ser^{473} and pS6 Ser$^{240-244}$ protein expression in 1 year old males and females. N = 4-5 mice per group. Data are shown as mean ± SEM. Statistical significance was determined by unpaired t-test. * $p < 0.05$; ** $p < 0.01$; *** $p < 0.0001$.

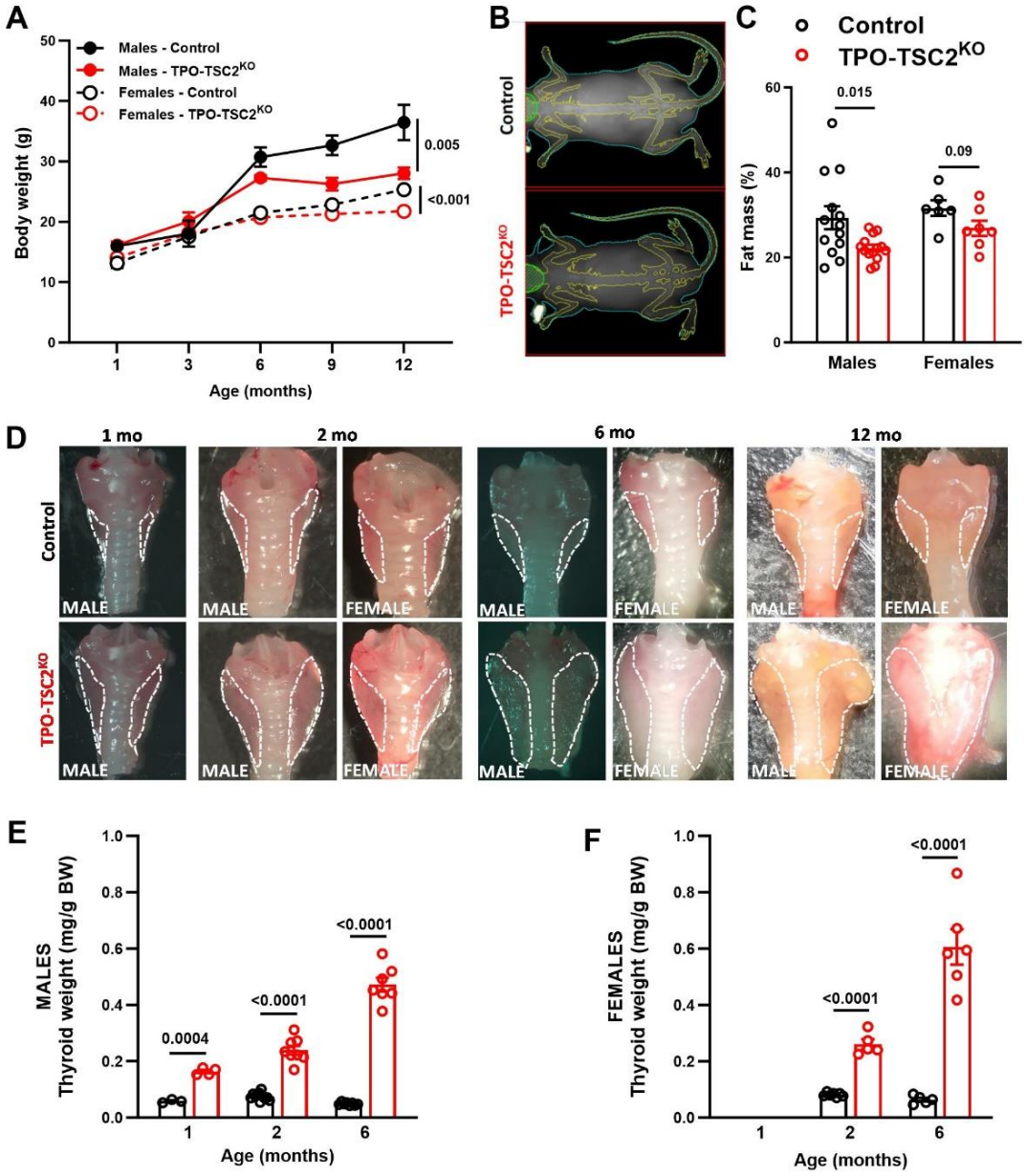

Figure 2. Overactivation of mTORC1 in thyrocytes leads to decreased body and fat mass and enlarged thyroid. (a) Body weight evolution during the first year of life in Control and TPO-TSC2^{KO} males and females. (b) Representative images and (c) Fat mass of 12 months old males and females evaluated by DEXA. (d) Photographs of thyroids at 1, 2, 6 and 12 months old males and females. (e) Thyroid mass normalized by body weight in males at 1, 2 and 6 months of age. (f) Thyroid mass normalized by body weight in females at 2 and 6 months of age. N = 5-10 mice per group. Data are shown as mean ± SEM. In A statistical significance was determined by two-way ANOVA (Tukey's multiple comparison correction). In C, E and F statistical significance was determined by unpaired t-test. P values are indicated when $p < 0.05$.

mTORC1 increases *thyrocyte hypertrophy and proliferation*

We next assessed the thyroid gland structure and thyrocyte proliferation to understand how mTORC1 promotes thyroid growth. We measured ~100 follicles of female mice and observed a 3-fold increase in the follicular area (Fig 3A and B). This was explained by a 2-fold increase in both colloid and epithelium (thyrocyte) areas (Fig 3C and D). These effects were also noticeable using the individual median values (Fig 3E and G). Indeed, follicle area frequency distribution analysis revealed that TPO-TSC2^{KO} mice have fewer small follicles (<1000 μm^2) but a higher number of follicles with areas between 3000 and 6000 μm^2 (Fig 3I). However, the epithelium-to-colloid ratio did not change (Fig 3H). Besides increasing in growth, mTORC1 enhanced thyrocyte proliferation assessed by Ki67 staining (Fig 4). The number of proliferating thyrocytes (TTF1$^+$Ki67$^+$ cells/TTF1$^+$ cells) was a 10-fold increase in female TPO-TSC2^{KO} mice compared to controls at 6 months of age (Fig 4A and B). Because cyclin D3 is critical for thyrocyte proliferation [57-60], we assessed its protein content and found that cyclin D3, but not D2, is increased in both males and females TPO-TSC2^{KO} mice (Fig 4C and D).

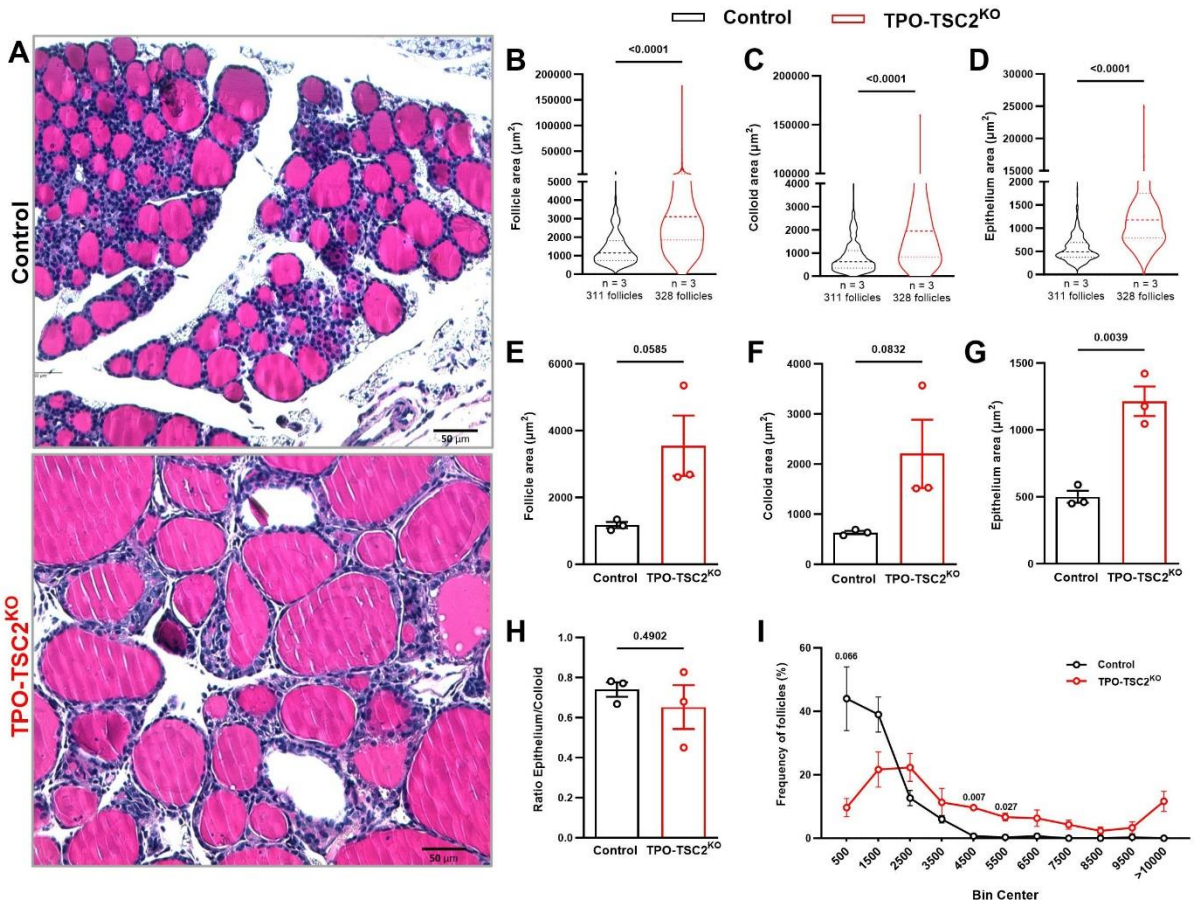

Figure 3. mTORC1 overactivation in thyrocytes leads to follicle enlargement. (a) Photomicrographs of thyroid gland histological sections of Control and TPO-TSC2 knockout mice. PAS staining. Scale bar: 50 µm (b) Distribution of the follicle area of single follicles. (c) Distribution of the colloid area of single follicles. (d) Distribution of the epithelium area of single follicles. (e) Median of follicle area. (f) Median of colloid area. (g) Median of epithelium area. (h) Ratio of epithelium area and colloid area. (i) Frequency distribution of follicles. In E, F and G data are shown as median ± SEM. N = 3 mice per group. Statistical significance was determined by unpaired t-test. P values are indicated when $p < 0.05$.

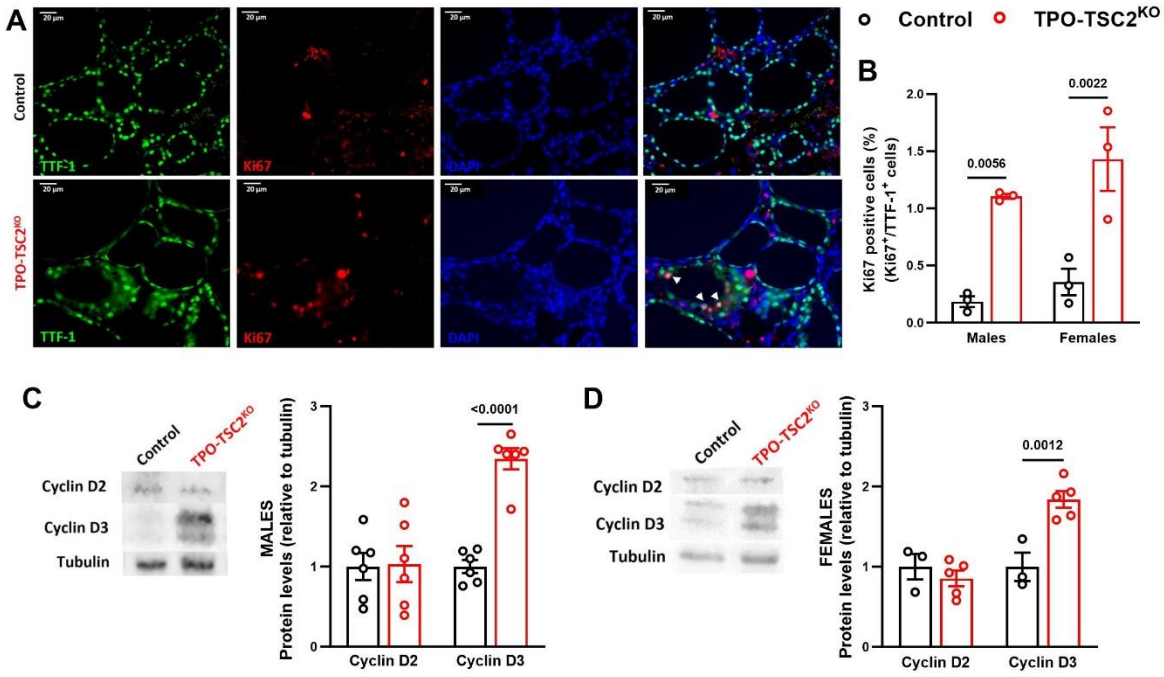

Figure 4. mTORC1 overactivation in thyroid causes thyrocyte proliferation. (a) Immunostaining for TTF-1 (green), Ki67 (red) and DAPI (blue) in thyroids from Control and TPO-TSC2 knockout mice at 6 months of age. Scale bar: 20 µM. Arrows indicate $Ki67^+/TTF\text{-}1^+$ cells. (b) Quantification of $Ki67^+/TTF\text{-}1^+$ cells. N = 3 mice per group. (c) Cyclin D2 and Cyclin D3 protein expression in thyroids of 6 months old males. (d) Cyclin D2 and Cyclin D3 protein expression in thyroids of 6 months old females. N = 3–6 mice per group. Data are shown as mean ± SEM. Statistical significance was determined by unpaired t-test. P values are indicated when $p < 0.05$.

mTORC1 regulates the expression of key regulatory genes in the thyroid gland

We next tested whether mTORC1 activation impacts gene expression in the thyrocytes at 2, 6, and 12 months of age in the TPO-TSC2^{KO} mice. As expected, TSC2 mRNA levels are 80-90% reduced in TPO-TSC2^{KO} mice of all ages and genders (Fig 5). Notably, NIS and TG mRNA levels are remarkably low at 6 and 12 months of age (males and females; Fig 5A-D). In addition, activation of mTORC1 promoted a remarkable decrease in NIS protein levels in 6-mo males and females (Fig 5E-F). TPO expression was normal at 2 months but decreased by 40% in females and males at 6 and 12 months (Fig 5A-D). While mTORC1 activation increased TSH receptor gene expression only in TPO-TSC2^{KO} males (Fig 5A and B), it increased the type 1 deiodinase (DIO1) in females at 6 months (Fig 5A and B). To evaluate if this modified gene expression profile was a function of mTORC1-mediated alteration of thyrocyte differentiation, we also measured the expression of the two main transcription factors that determine thyrocyte identity and maturation, PAX8 and TTF1[61]. We did not observe any difference in the mRNA levels of these genes in males or females TPO-TSC2^{KO} mice at any age (Fig 5).

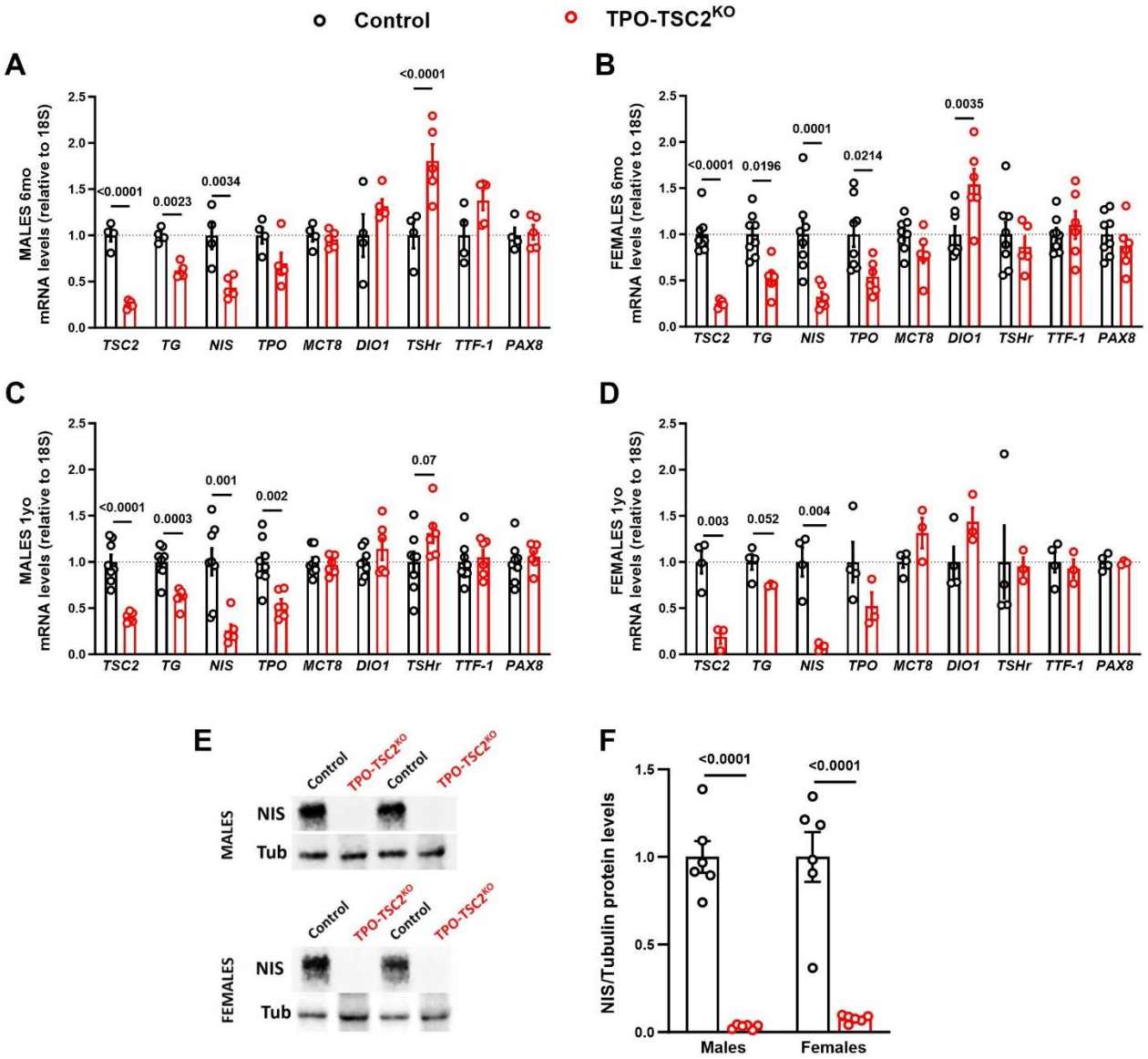

Figure 5. mTORC1 overactivation impairs thyrocyte function. (a) mRNA levels of thyroid markers in 6 months old males. (b) mRNA levels of thyroid markers in 6 months old females. (c) mRNA levels of thyroid markers in 1 year old males. (d) mRNA levels of thyroid markers in 1 year old females. (e) Representative western blots and (f) quantitative determination of NIS protein expression in males and females at 6 months of age. N = 3–8 mice per group. Data are shown as mean ± SEM. Statistical significance was determined by unpaired t-test. P values are indicated when $p < 0.05$.

Prolonged mTORC1 activation impairs thyroid function

Although mTORC1 activation altered the expression of key genes involved in thyroid hormone synthesis, total T_4, T_3, and TSH plasma levels were normal in 2-month-old male TPO-TSC2^{KO} mice (Table 3). At 6 months of age, both male and female TPO-TSC2^{KO} mice had higher TSH levels with a trend to lower levels of T_4 ($p < 0.07$ and $p < 0.06$, respectively; Tables 3 and 4). TPO-TSC2^{KO} mice aged one year exhibited higher TSH and reduced T_4 levels in both genders (Tables 3 and 4). In contrast, circulating T_3 levels in TPO-TSC2^{KO} mice were similar to controls throughout life.

TABLE 3. Plasma TSH, T_4, and T_3 in Control and TPO-TSC2^{KO} male mice

Age (months)		TSH (ng/mL)	Total T_4 (ng/mL)	Total T_3 (ng/mL)
2	**Control**	37.61 ± 8.76 (5)	74.2 ± 3.3 (9)	2.12 ± 0.04 (9)
	TPO-TSC2^{KO}	46.4 ± 10 (6)	70.2 ± 3.5 (8)	1.99 ± 0.08 (8)
6	**Control**	39.5 ± 9.5 (10)	93.3 ± 6.3 (4)	0.88 ± 0.008 (4)
	TPO-TSC2^{KO}	82.8 ± 17.7* (11)	76.2 ± 5.1$^{p=0.07}$ (8)	0.89 ± 0.008 (7)
12	**Control**	69.2 ± 8.2 (4)	106.5 ± 14.6 (7)	1.09 ± 0.043 (10)
	TPO-TSC2^{KO}	203.6 ± 42.4* (8)	75.7 ± 4.7$^{p=0.08}$ (6)	1.03 ± 0.043 (8)

Data are shown in Mean ± SEM. * $p < 0.05$ *vs* Littermate controls at the same age.
Sample sizes are given in parentheses.

TABLE 4. Plasma TSH, T_4, and T_3 in Control and TPO-TSC2^{KO} female mice

Age (months)		TSH (ng/mL)	Total T_4 (ng/mL)	Total T_3 (ng/mL)
6	**Control**	32.2 ± 7.13 (10)	118.7 ± 7.7 (6)	0.86 ± 0.013 (5)
	TPO-TSC2^{KO}	71.1 ± 12.5* (8)	100.2 ± 4.9 $^{p=0.06}$ (7)	0.87 ± 0.005 (6)
12	**Control**	36.4 ± 10.2 (5)	140.6 ± 14.1 (4)	0.94 ± 0.008 (4)
	TPO-TSC2^{KO}	160.8 ± 13.9*** (6)	111.9 ± 6.4* (4)	0.94 ± 0.007 (4)

Data are shown in Mean ± SEM. * $p < 0.05$ and *** $p < 0.0001$ *vs* Littermate controls at the same age.
Sample sizes are given in parentheses.

Pharmacological Inhibition of mTORC1 reverses the **TPO-TSC2^{KO}** *phenotype*

To further demonstrate that the TPO-TSC2^{KO} mice phenotype was due to enhanced mTORC1 activity in the thyrocytes, we pharmacologically inhibited mTORC1 with daily injections of Rapamycin, a well-known inhibitor of mTORC1. Both, control and TPO-TSC2^{KO} male mice received Rapamycin (2 mg/kg *ip*) for 5 weeks from weaning (3 weeks old) until 2 months of age (Fig 6A). Rapamycin treatment successfully blocked mTORC1 activity (Fig 6B) and fully blunted mTORC1-mediated thyroid mass growth observed in the TPO-TSC2^{KO} mice (Fig 6C). At the molecular level, Rapamycin administration reversed the changes in the expression of TPO, NIS, Dio1, and TSHr (Fig 6D vs 5A). Total T_3, T_4, and TSH levels were not different between control and TPO-TSC2^{KO} mice at 2 months of age (Fig 6E) as expected for this age. However, we detected a decrease in blood T_4 induced by Rapamycin treatment, suggesting impaired thyroid function (Fig 6E). These results suggest that the increase in thyroid growth and thyrocyte proliferation observed in TPO-TSC2^{KO} mice occurs independently of TSH.

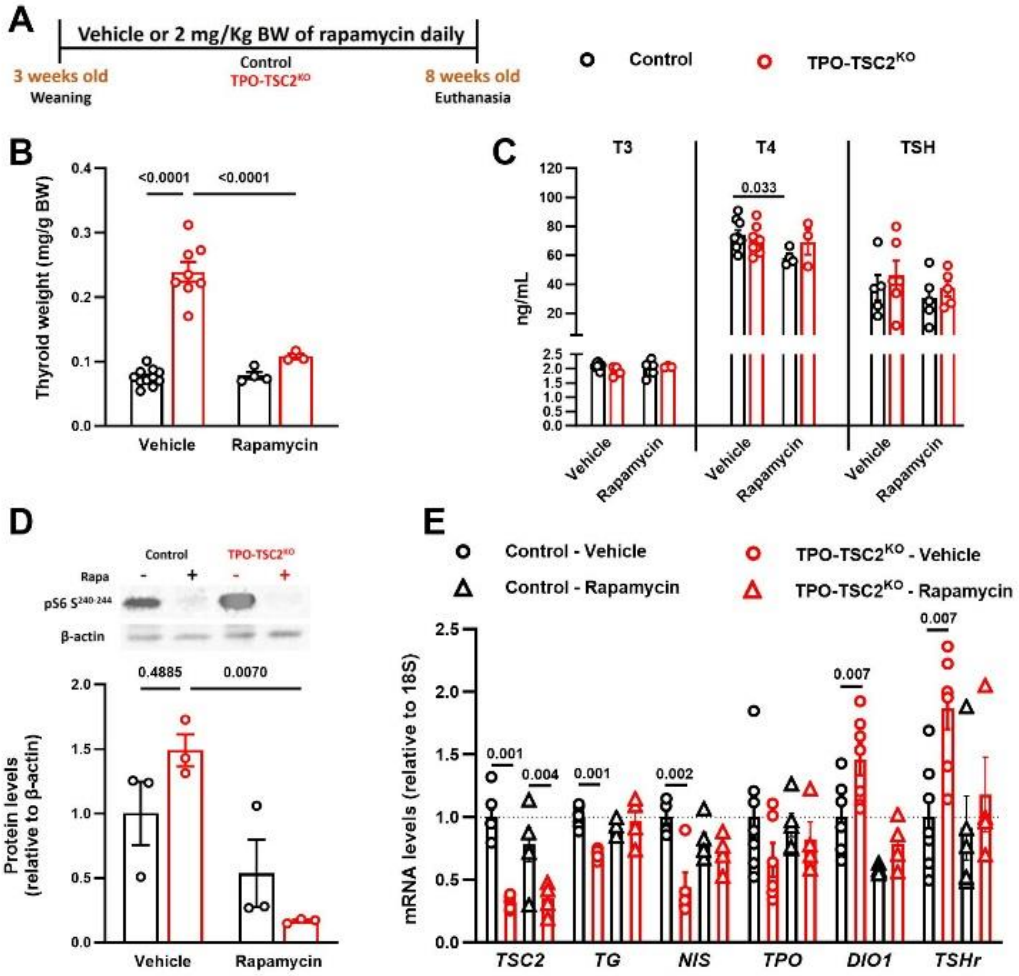

Figure 6. Rapamycin treatment blocks thyroid mass expansion and gene regulation in the TPO-TSC2^{KO}. (a) TPO-TSC2 knockout male mice were treated daily with 2 mg/Kg BW Rapa from 3 to 8 weeks of age. (b) Thyroid weight normalized by body weight in males. (c) Total T3, total T4 and TSH levels. (d) Thyroid pS6 protein levels. (e) Thyroid mRNA levels. N = 3–6 mice per group. Data are shown as mean ± SEM. Statistical significance was determined by unpaired t-test. P values are indicated when $p < 0.05$.

Old* TPO-TSC2^{KO} *mice present aberrant thyroid follicles, inflammation, and tumors

Overactivation of mTORC1 led to the development of abnormal thyroids, characterized by multiple layers of thyrocytes and colloid between them (Fig 7A-C). Microscopic examination of thyroids from TPO-TSC2 knockout mice revealed nodular thyroid follicular disease with extensive cystic changes. Most of the follicles were lined by flattened or round oval follicular cells. Rare follicles exhibited focal centripetal papillary hyperplasia, and there were small areas with follicle breakdown with acute inflammation and histiocytic type reaction. After 12 months of age, mice with mTORC1 overactivation in thyroid developed tumors (Fig 7D-E).

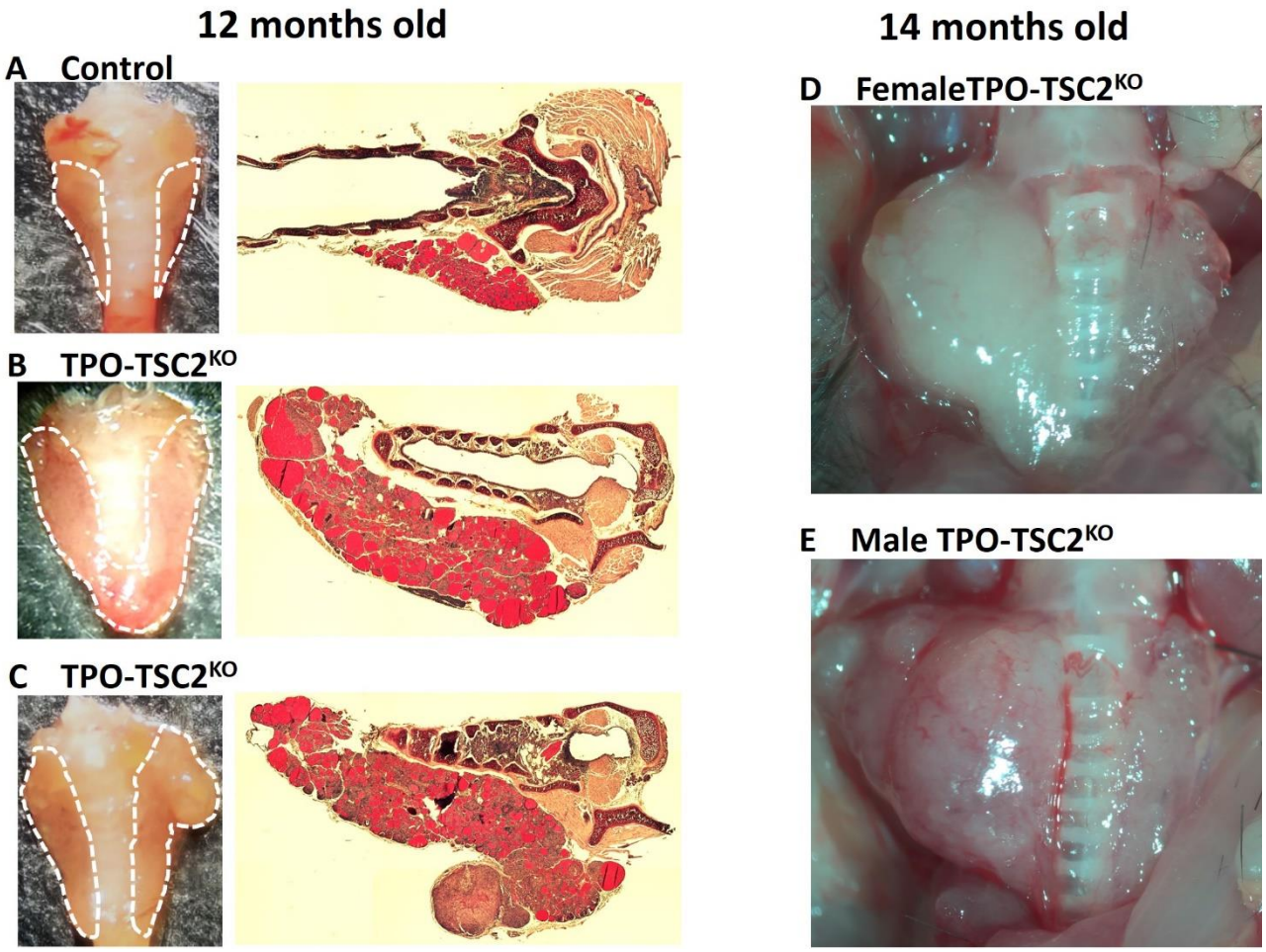

Figure 7. 12 month-old or older TPO-TSC2^{KO} mice present aberrant thyroids. (a) Photo and photomicrographs of thyroid gland histological sections of 12 months old Control mice. (b) Photo and photomicrographs of thyroid gland histological sections of 12 months old TPO-TSC2^{KO} mice. (c) Photo and photomicrographs of thyroid gland histological sections of 12 months old TPO-TSC2^{KO} mice with a tumor. PAS staining. (d) Thyroid tumor in a 14 months old TPO-TSC2^{KO} female. (e) Thyroid tumor in a 14 months old TPO-TSC2^{KO} male.

DISCUSSION

Our study has demonstrated that the overactivation of mTORC1 in thyrocytes leads to an increase in thyroid weight, the development of larger follicles characterized by more colloid and a larger epithelium, and an elevated rate of proliferation. We also found that administering rapamycin from weaning until the age of 8 weeks effectively mitigated this thyroid growth. It is well-established that the PI3K-Akt-mTORC pathway plays a pivotal role in cell growth and proliferation. In the 1990s, it was established that treatment of cultured sheep thyrocytes with insulin and IGF-1 increased the proliferation induced by TSH [62]. Supporting this data, mice with an IGF-1 receptor deletion in thyrocytes did not exhibit an increase in thyrocyte area and in the thyroid epithelium height following TSH injections, unlike their control counterparts. These IGF-1 receptor knockout mice did not develop an enlarged thyroid after goiter induction with sodium perchlorate and methimazole in their drinking water. The involvement of mTOR pathway in this process is suggested because the goitrogenic condition failed to increase the p-mTOR and p-S6 levels in these IGF-1 receptor knockout mice [24]. However, double knockout mice for IGF-1 and insulin receptor in the thyroid (DTIRKO) presented a different phenotype. Neonatal DTIRKO mice had smaller thyroids, mirroring defective folliculogenesis. By contrast, by postnatal day 14, the absence of IR and IGF-1R paradoxically induced thyrocyte proliferation, which was mediated by mTOR-dependent signaling pathways [26]. The authors speculated that the elevated circulating levels of TSH observed in these mice at postnatal day 14 could compensate for the loss of IGF-1R and IR signaling and be responsible for the thyroid hyperplasia. The significant role of mTORC1 in thyrocyte proliferation is evident because the increase in rat thyrocyte proliferation caused by TSH, as assessed by BrDU incorporation, was blunted when the thyrocytes were pre-treated with rapamycin [63]. Moreover, chronic *in vivo* treatment of mice with RAD001 (Everolimus), an mTORC1 inhibitor, during goitrogenic stimulation also abrogated the

hyperplastic thyrocyte response to TSH [27]. This data suggests that TSH and insulin/IGF-1 act synergically through PI3K-Akt-mTOR pathway to induce thyrocyte proliferation.

The role of mTORC1 pathway in the synthesis and secretion of thyroid hormones remains somewhat ambiguous. A significant portion of research has concentrated on the interaction between mTORC1 and NIS expression. Some literature suggests that, contrary to observations in proliferation, TSH and insulin/IGF-1 exert opposing effects. In FRTL-5 cell culture, IGF-I did not alter NIS mRNA levels but did inhibit TSH- and forskolin induced NIS mRNA expression in a dose-dependent manner. Notably, PI3K inhibition blocked the IGF-I repression of TSH induced NIS mRNA and protein levels [12]. In PCCL3 cells, a dose-dependent stimulation of iodide uptake by rapamycin was observed in the presence of TSH. In these cells, without TSH, NIS expression was low and unaffected by rapamycin treatment. However, when TSH is present in the culture medium, NIS expression is increased and insulin significantly decreased NIS expression. This effect was counteracted by rapamycin, which restored NIS expression [15]. On the other hand, co-treatment of human thyrocytes with TSH/IGF-1 produced additive effects on TG, TPO, DIO2 and NIS mRNA levels. The IGF-1R tyrosine kinase inhibitor linsitinib inhibited the TSH-stimulated upregulation of NIS but not TG, suggesting that NIS regulation is partly IGF-1R dependent and occurs via receptor crosstalk [42]. The discrepancies between these data may be attributed to the *in vitro* conditions that do not permit thyrocyte organization as follicles and thus do not fully represent thyroid gland physiology [44].

In vivo data demonstrating the impact of the PI3K-Akt-mTOR pathway on thyroid gland physiology is limited. It has been observed that mTOR inhibition with Everolimus significantly increased thyroid iodide uptake by 50% related to control in Wistar rats [15]. This evidence suggests that mTOR inhibition regulates iodide uptake not only *in vitro* but also *in vivo*. Moreover, mice with deletion of the IGF-1 receptor in thyrocytes exhibited lower expression of TPO and MCT8. By 6 weeks of age, these mice displayed lower T_4 levels and higher TSH levels, and their T_4 secretion was impaired post-TSH induction [24]. A similar hypothyroid-like phenotype in IGF-1 receptor knockout mice was seen by Muller et al [25]. Our findings corroborate these observations. We observed that mTORC1 overactivation in thyrocytes led to a decrease in mRNA expression of NIS, Tg and TPO in males and females aged 2, 6 and 12 months. Protein levels of NIS were also decreased in 6 months old males and females. Interestingly, the decrease in gene expression was prevented when TPO-TSC2^{KO} received daily injections of rapamycin from weaning. At the age of 2 months, we observed no difference in T_4, T_3 and TSH levels between Control and TPO-TSC2^{KO} mice. However, there was a trend towards decreasing T_4 levels in 6 and 12-month-old mice, and increased TSH levels were observed in males and females of the same ages. In summary, the observed decrease in gene expression in 2-month-old TPO-TSC2^{KO} mice, regardless of any changes in hormone levels, along with the decreased gene expression in 6 and 12-month-old mice despite increased TSH levels, and the prevention of these gene alterations with rapamycin treatment all suggest a significant role of mTORC1 in controlling the synthesis and/or secretion of thyroid hormones. Importantly, mRNA levels of the TSH receptor increased in males TPO-TSC2^{KO} mice aged 2, 6 and 12 months. Additionally, mRNA levels of DIO1 increased in females knockout aged 6 months and male knockouts aged 2 months but remained unaffected at other ages and sexes studies. This indicates that mTORC1 activation does not affect TSH signaling.

The role of mTOR in thyroid cancer is well established. Differentiated thyroid carcinoma (DTC) arises from thyroid follicular cells and represents more than 90% of all cases of thyroid cancer. DTC comprises papillary thyroid carcinoma (PTC) and follicular thyroid carcinoma (FTC), with PTC being the most prevalent type [64]. PTC carries an overall good prognosis (overall survival rates of >95% at 25 years) after being treated with surgery followed by radioactive iodine (RAI) therapy [65, 66]. However, 5-10% of the PTCs develop regional recurrences or distant metastasis and, of these, a big part become refractory to RAI therapy [66]. There is increasing evidence that the mTOR pathway plays a role in these poor outcomes in PTC. In a Portuguese cohort, pmTOR expression was associated with distant metastases and persistence of disease. Importantly, cases with greater expression of pmTOR were submitted to more ^{131}I treatments and a greater cumulative dose of radioactive iodine [67]. For instance, oncogenic mutations in the PI3K/Akt/mTORC1 pathway are associated with a worse prognosis in patients with BRAFV600E-driven papillary cancer, and these mutations are independent predictors of mortality [28]. However, mTORC2 also seems involved in the progression of thyroid cancer. Ahmed et al (2014) found that active mTORC1 was present in 81% of PTC samples and active mTORC2 was present in 39% of PTC samples. Co-expression of mTORC1 and mTORC2 activity was seen in 32.5% of the PTC studied. *In vitro*, Torin2, an inhibitor of mTORC1 and mTORC2, inhibited cell viability and induced caspase-dependent apoptosis in PTC cells [33]. Finally, the impact of each mTOR complex was also studied by treating cancer thyroid cell lines with RAD001 and Torin2. Treatment with RAD001 did not increase NIS mRNA levels, whereas Torin2 caused a ~6 fold increase in NIS mRNA expression in the TPC1 cell line. In PTC,

phospho-mTOR activation may lead to the activation of the mTORC2 complex [29]. This data implies that mTORC2, besides mTORC1, also plays a role in thyroid cancer.

Our study revealed that mTORC1 overactivation led to the development of cysts and tumors in mice aged 12 months or older. Typically, TPO-TSC2^{KO} mice exhibited an enlarged thyroid, nodular thyroid follicular disease with focally cystic follicles, and extensive follicular proliferation with papillary centripetal follicular proliferation, which was associated with lymphocytic thyroiditis. Interestingly, some TPO-TSC2^{KO} thyroids showed a large area with oncocytic changes in the follicular cells. These cells had very large nuclei with pleomorphic and bizarre features, which are morphologically consistent with an oncocytic type carcinoma. However no invasive component or lymphatic invasion was identified. Intriguingly, double knockout mice for IR and IGF-1R in thyroid also present PTC-like lesions as they aged [26]. The authors posited that defective IR/IGF-1R signaling in thyrocytes could lead to changes in nutrient availability, such as decreased glucose utilization and increased amino acid availability, resulting in the direct activation of mTOR. These findings confirm mTORC1 pathway involvement in thyroid carcinogenesis.

CONCLUSION

Our study concludes that mTORC1 not only plays a pivotal role in controlling thyrocyte proliferation but also significantly influences thyrocyte function. Based on the results presented, we conclude that the activation of mTORC1 pathway can decrease the expression of NIS, TPO and TG, ultimately to reduced T_4 secretion. Future research will be directed towards identifying the specific intracellular targets of mTORC1 that mediate downregulation of thyroid hormone synthesis genes, and investigating whether mTORC1 is involved in thyroid hormone secretion.

REFERENCES

1. Meng X, Xu S, Chen G, Derwahl M, Liu C. Metformin and thyroid disease. J Endocrinol. 2017;233(1):R43-R51. doi: 10.1530/JOE-16-0450. PubMed PMID: 28196954.
2. Biondi B, Kahaly GJ, Robertson RP. Thyroid Dysfunction and Diabetes Mellitus: Two Closely Associated Disorders. Endocr Rev. 2019;40(3):789-824. doi: 10.1210/er.2018-00163. PubMed PMID: 30649221; PMCID: PMC6507635.
3. Alexander EK, Cibas ES. Diagnosis of thyroid nodules. Lancet Diabetes Endocrinol. 2022;10(7):533-9. Epub 2022/06/26. doi: 10.1016/S2213-8587(22)00101-2. PubMed PMID: 35752200.
4. Haugen BR, Alexander EK, Bible KC, Doherty GM, Mandel SJ, Nikiforov YE, Pacini F, Randolph GW, Sawka AM, Schlumberger M, Schuff KG, Sherman SI, Sosa JA, Steward DL, Tuttle RM, Wartofsky L. 2015 American Thyroid Association Management Guidelines for Adult Patients with Thyroid Nodules and Differentiated Thyroid Cancer: The American Thyroid Association Guidelines Task Force on Thyroid Nodules and Differentiated Thyroid Cancer. Thyroid. 2016;26(1):1-133. Epub 2015/10/16. doi: 10.1089/thy.2015.0020. PubMed PMID: 26462967; PMCID: PMC4739132.
5. Gursoy A. Rising thyroid cancer incidence in the world might be related to insulin resistance. Med Hypotheses. 2010;74(1):35-6. Epub 2009/09/02. doi: 10.1016/j.mehy.2009.08.021. PubMed PMID: 19720470.
6. Vassart G, Dumont JE. The thyrotropin receptor and the regulation of thyrocyte function and growth. Endocr Rev. 1992;13(3):596-611. doi: 10.1210/edrv-13-3-596. PubMed PMID: 1425489.
7. Laglia G, Zeiger MA, Leipricht A, Caturegli P, Levine MA, Kohn LD, Saji M. Increased cyclic adenosine 3',5'-monophosphate inhibits G protein-coupled activation of phospholipase C in rat FRTL-5 thyroid cells. Endocrinology. 1996;137(8):3170-6. doi: 10.1210/endo.137.8.8754735. PubMed PMID: 8754735.
8. Song Y, Massart C, Chico-Galdo V, Jin L, De Maertelaer V, Decoster C, Dumont JE, Van Sande J. Species specific thyroid signal transduction: conserved physiology, divergent mechanisms. Mol Cell Endocrinol. 2010;319(1-2):56-62. Epub 20100128. doi: 10.1016/j.mce.2010.01.024. PubMed PMID: 20109522.
9. Colin IM, Denef JF, Lengele B, Many MC, Gerard AC. Recent insights into the cell biology of thyroid angiofollicular units. Endocr Rev. 2013;34(2):209-38. Epub 2013/01/26. doi: 10.1210/er.2012-1015. PubMed PMID: 23349248; PMCID: PMC3610675.
10. Rousset B, Dupuy C, Miot F, Dumont J. Chapter 2 Thyroid Hormone Synthesis And Secretion. In: Feingold KR, Anawalt B, Blackman MR, Boyce A, Chrousos G, Corpas E, de Herder WW, Dhatariya K, Dungan K, Hofland J, Kalra S, Kaltsas G, Kapoor N, Koch C, Kopp P, Korbonits M, Kovacs CS, Kuohung W, Laferrere B, Levy M, McGee EA, McLachlan R, New M, Purnell J, Sahay R, Shah AS, Singer F, Sperling MA, Stratakis CA, Trence DL, Wilson DP, editors. Endotext. South Dartmouth (MA)2000.

11. Coulonval K, Vandeput F, Stein RC, Kozma SC, Lamy F, Dumont JE. Phosphatidylinositol 3-kinase, protein kinase B and ribosomal S6 kinases in the stimulation of thyroid epithelial cell proliferation by cAMP and growth factors in the presence of insulin. Biochem J. 2000;348 Pt 2(Pt 2):351-8. PubMed PMID: 10816429; PMCID: PMC1221073.
12. Garcia B, Santisteban P. PI3K is involved in the IGF-I inhibition of TSH-induced sodium/iodide symporter gene expression. Mol Endocrinol. 2002;16(2):342-52. Epub 2002/01/31. doi: 10.1210/mend.16.2.0774. PubMed PMID: 11818505.
13. Kimura T, Van Keymeulen A, Golstein J, Fusco A, Dumont JE, Roger PP. Regulation of thyroid cell proliferation by TSH and other factors: a critical evaluation of in vitro models. Endocr Rev. 2001;22(5):631-56. Epub 2001/10/06. doi: 10.1210/edrv.22.5.0444. PubMed PMID: 11588145.
14. Bellacosa A, Kumar CC, Di Cristofano A, Testa JR. Activation of AKT kinases in cancer: implications for therapeutic targeting. Adv Cancer Res. 2005;94:29-86. doi: 10.1016/S0065-230X(05)94002-5. PubMed PMID: 16095999.
15. de Souza EC, Padron AS, Braga WM, de Andrade BM, Vaisman M, Nasciutti LE, Ferreira AC, de Carvalho DP. MTOR downregulates iodide uptake in thyrocytes. J Endocrinol. 2010;206(1):113-20. Epub 2010/04/16. doi: 10.1677/JOE-09-0436. PubMed PMID: 20392814.
16. Sarbassov DD, Ali SM, Sabatini DM. Growing roles for the mTOR pathway. Curr Opin Cell Biol. 2005;17(6):596-603. Epub 20051013. doi: 10.1016/j.ceb.2005.09.009. PubMed PMID: 16226444.
17. Liu GY, Sabatini DM. mTOR at the nexus of nutrition, growth, ageing and disease. Nat Rev Mol Cell Biol. 2020;21(4):183-203. doi: 10.1038/s41580-019-0199-y. PubMed PMID: 31937935; PMCID: PMC7102936.
18. Gingras AC, Gygi SP, Raught B, Polakiewicz RD, Abraham RT, Hoekstra MF, Aebersold R, Sonenberg N. Regulation of 4E-BP1 phosphorylation: a novel two-step mechanism. Genes Dev. 1999;13(11):1422-37. Epub 1999/06/11. doi: 10.1101/gad.13.11.1422. PubMed PMID: 10364159; PMCID: PMC316780.
19. Hara K, Yonezawa K, Kozlowski MT, Sugimoto T, Andrabi K, Weng QP, Kasuga M, Nishimoto I, Avruch J. Regulation of eIF-4E BP1 phosphorylation by mTOR. J Biol Chem. 1997;272(42):26457-63. Epub 1997/10/23. doi: 10.1074/jbc.272.42.26457. PubMed PMID: 9334222.
20. Chauvin C, Koka V, Nouschi A, Mieulet V, Hoareau-Aveilla C, Dreazen A, Cagnard N, Carpentier W, Kiss T, Meyuhas O, Pende M. Ribosomal protein S6 kinase activity controls the ribosome biogenesis transcriptional program. Oncogene. 2014;33(4):474-83. Epub 2013/01/16. doi: 10.1038/onc.2012.606. PubMed PMID: 23318442.
21. Hannan KM, Brandenburger Y, Jenkins A, Sharkey K, Cavanaugh A, Rothblum L, Moss T, Poortinga G, McArthur GA, Pearson RB, Hannan RD. mTOR-dependent regulation of ribosomal gene transcription requires S6K1 and is mediated by phosphorylation of the carboxy-terminal activation domain of the nucleolar transcription factor UBF. Mol Cell Biol. 2003;23(23):8862-77. Epub 2003/11/13. doi: 10.1128/MCB.23.23.8862-8877.2003. PubMed PMID: 14612424; PMCID: PMC262650.
22. Smith TJ. Insulin-Like Growth Factor Pathway and the Thyroid. Front Endocrinol (Lausanne). 2021;12:653627. Epub 2021/06/22. doi: 10.3389/fendo.2021.653627. PubMed PMID: 34149612; PMCID: PMC8212127.
23. Krieger CC, Neumann S, Gershengorn MC. TSH/IGF1 receptor crosstalk: Mechanism and clinical implications. Pharmacol Ther. 2020;209:107502. Epub 2020/02/18. doi: 10.1016/j.pharmthera.2020.107502. PubMed PMID: 32061922; PMCID: PMC7187798.
24. Ock S, Ahn J, Lee SH, Kang H, Offermanns S, Ahn HY, Jo YS, Shong M, Cho BY, Jo D, Abel ED, Lee TJ, Park WJ, Lee IK, Kim J. IGF-1 receptor deficiency in thyrocytes impairs thyroid hormone secretion and completely inhibits TSH-stimulated goiter. FASEB J. 2013;27(12):4899-908. Epub 2013/08/29. doi: 10.1096/fj.13-231381. PubMed PMID: 23982142.
25. Muller K, Fuhrer D, Mittag J, Kloting N, Bluher M, Weiss RE, Many MC, Schmid KW, Krohn K. TSH compensates thyroid-specific IGF-I receptor knockout and causes papillary thyroid hyperplasia. Mol Endocrinol. 2011;25(11):1867-79. Epub 2011/10/08. doi: 10.1210/me.2011-0065. PubMed PMID: 21980075; PMCID: PMC5417177.
26. Ock S, Ahn J, Lee SH, Kim HM, Kang H, Kim YK, Kook H, Park WJ, Kim S, Kimura S, Jung CK, Shong M, Holzenberger M, Abel ED, Lee TJ, Cho BY, Kim HS, Kim J. Thyrocyte-specific deletion of insulin and IGF-1 receptors induces papillary thyroid carcinoma-like lesions through EGFR pathway activation. Int J Cancer. 2018;143(10):2458-69. Epub 2018/08/03. doi: 10.1002/ijc.31779. PubMed PMID: 30070361; PMCID: PMC6698377.
27. Brewer C, Yeager N, Di Cristofano A. Thyroid-stimulating hormone initiated proliferative signals converge in vivo on the mTOR kinase without activating AKT. Cancer Res. 2007;67(17):8002-6. Epub 2007/09/07. doi: 10.1158/0008-5472.CAN-07-2471. PubMed PMID: 17804710.
28. Pappa T, Ahmadi S, Marqusee E, Johnson HL, Nehs MA, Cho NL, Barletta JA, Lorch JH, Doherty GM, Lindeman NI, Alexander EK, Landa I. Oncogenic Mutations in PI3K/AKT/mTOR Pathway Effectors Associate with Worse Prognosis in

BRAF(V600E) -Driven Papillary Thyroid Cancer Patients. Clin Cancer Res. 2021;27(15):4256-64. Epub 2021/06/06. doi: 10.1158/1078-0432.CCR-21-0874. PubMed PMID: 34088725.
29. Tavares C, Eloy C, Melo M, Gaspar da Rocha A, Pestana A, Batista R, Bueno Ferreira L, Rios E, Sobrinho Simoes M, Soares P. mTOR Pathway in Papillary Thyroid Carcinoma: Different Contributions of mTORC1 and mTORC2 Complexes for Tumor Behavior and SLC5A5 mRNA Expression. Int J Mol Sci. 2018;19(5). Epub 2018/05/15. doi: 10.3390/ijms19051448. PubMed PMID: 29757257; PMCID: PMC5983778.
30. Faustino A, Couto JP, Populo H, Rocha AS, Pardal F, Cameselle-Teijeiro JM, Lopes JM, Sobrinho-Simoes M, Soares P. mTOR pathway overactivation in BRAF mutated papillary thyroid carcinoma. J Clin Endocrinol Metab. 2012;97(7):E1139-49. Epub 2012/05/03. doi: 10.1210/jc.2011-2748. PubMed PMID: 22549934.
31. Landa I, Ibrahimpasic T, Boucai L, Sinha R, Knauf JA, Shah RH, Dogan S, Ricarte-Filho JC, Krishnamoorthy GP, Xu B, Schultz N, Berger MF, Sander C, Taylor BS, Ghossein R, Ganly I, Fagin JA. Genomic and transcriptomic hallmarks of poorly differentiated and anaplastic thyroid cancers. J Clin Invest. 2016;126(3):1052-66. Epub 2016/02/16. doi: 10.1172/JCI85271. PubMed PMID: 26878173; PMCID: PMC4767360.
32. Sadowski SM, Boufraqech M, Zhang L, Mehta A, Kapur P, Zhang Y, Li Z, Shen M, Kebebew E. Torin2 targets dysregulated pathways in anaplastic thyroid cancer and inhibits tumor growth and metastasis. Oncotarget. 2015;6(20):18038-49. Epub 2015/05/07. doi: 10.18632/oncotarget.3833. PubMed PMID: 25945839; PMCID: PMC4627234.
33. Ahmed M, Hussain AR, Bavi P, Ahmed SO, Al Sobhi SS, Al-Dayel F, Uddin S, Al-Kuraya KS. High prevalence of mTOR complex activity can be targeted using Torin2 in papillary thyroid carcinoma. Carcinogenesis. 2014;35(7):1564-72. Epub 2014/03/04. doi: 10.1093/carcin/bgu051. PubMed PMID: 24583924.
34. Kouvaraki MA, Liakou C, Paraschi A, Dimas K, Patsouris E, Tseleni-Balafouta S, Rassidakis GZ, Moraitis D. Activation of mTOR signaling in medullary and aggressive papillary thyroid carcinomas. Surgery. 2011;150(6):1258-65. Epub 2011/12/06. doi: 10.1016/j.surg.2011.09.022. PubMed PMID: 22136849.
35. Hanna GJ, Busaidy NL, Chau NG, Wirth LJ, Barletta JA, Calles A, Haddad RI, Kraft S, Cabanillas ME, Rabinowits G, O'Neill A, Limaye SA, Alexander EK, Moore FD, Jr., Misiwkeiwicz K, Thomas T, Nehs M, Marqusee E, Lee SL, Janne PA, Lorch JH. Genomic Correlates of Response to Everolimus in Aggressive Radioiodine-refractory Thyroid Cancer: A Phase II Study. Clin Cancer Res. 2018;24(7):1546-53. Epub 2018/01/06. doi: 10.1158/1078-0432.CCR-17-2297. PubMed PMID: 29301825.
36. Harris EJ, Hanna GJ, Chau NG, Rabinowits G, Haddad RI, Margalit DN, Schoenfeld JD, Tishler RB, Barletta JA, Nehs M, Janne PA, Huang J, Groden P, Kacew A, Lorch JH. Everolimus in anaplastic thyroid cancer: A case series. Journal of Clinical Oncology. 2018;36(15). doi: DOI 10.1200/JCO.2018.36.15_suppl.e18112. PubMed PMID: WOS:000442916005663.
37. McFadden DG, Vernon A, Santiago PM, Martinez-McFaline R, Bhutkar A, Crowley DM, McMahon M, Sadow PM, Jacks T. p53 constrains progression to anaplastic thyroid carcinoma in a Braf-mutant mouse model of papillary thyroid cancer. Proc Natl Acad Sci U S A. 2014;111(16):E1600-9. Epub 2014/04/09. doi: 10.1073/pnas.1404357111. PubMed PMID: 24711431; PMCID: PMC4000830.
38. Vanden Borre P, Gunda V, McFadden DG, Sadow PM, Varmeh S, Bernasconi M, Parangi S. Combined BRAF(V600E)- and SRC-inhibition induces apoptosis, evokes an immune response and reduces tumor growth in an immunocompetent orthotopic mouse model of anaplastic thyroid cancer. Oncotarget. 2014;5(12):3996-4010. Epub 2014/07/06. doi: 10.18632/oncotarget.2130. PubMed PMID: 24994118; PMCID: PMC4147301.
39. Papewalis C, Wuttke M, Schinner S, Willenberg HS, Baran AM, Scherbaum WA, Schott M. Role of the novel mTOR inhibitor RAD001 (everolimus) in anaplastic thyroid cancer. Horm Metab Res. 2009;41(10):752-6. Epub 2009/06/11. doi: 10.1055/s-0029-1224116. PubMed PMID: 19513966.
40. Morale MG, Tamura RE, Rubio IGS. Metformin and Cancer Hallmarks: Molecular Mechanisms in Thyroid, Prostate and Head and Neck Cancer Models. Biomolecules. 2022;12(3). Epub 2022/03/26. doi: 10.3390/biom12030357. PubMed PMID: 35327549; PMCID: PMC8945547.
41. Krieger CC, Perry JD, Morgan SJ, Kahaly GJ, Gershengorn MC. TSH/IGF-1 Receptor Cross-Talk Rapidly Activates Extracellular Signal-Regulated Kinases in Multiple Cell Types. Endocrinology. 2017;158(10):3676-83. Epub 2017/09/25. doi: 10.1210/en.2017-00528. PubMed PMID: 28938449; PMCID: PMC5659693.
42. Morgan SJ, Neumann S, Marcus-Samuels B, Gershengorn MC. Thyrotropin and Insulin-Like Growth Factor 1 Receptor Crosstalk Upregulates Sodium-Iodide Symporter Expression in Primary Cultures of Human Thyrocytes. Thyroid. 2016;26(12):1794-803. Epub 2016/10/19. doi: 10.1089/thy.2016.0323. PubMed PMID: 27638195; PMCID: PMC5175432.

43. Zaballos MA, Garcia B, Santisteban P. Gbetagamma dimers released in response to thyrotropin activate phosphoinositide 3-kinase and regulate gene expression in thyroid cells. Mol Endocrinol. 2008;22(5):1183-99. Epub 2008/01/19. doi: 10.1210/me.2007-0093. PubMed PMID: 18202153; PMCID: PMC5419518.
44. Bernier-Valentin F, Trouttet-Masson S, Rabilloud R, Selmi-Ruby S, Rousset B. Three-dimensional organization of thyroid cells into follicle structures is a pivotal factor in the control of sodium/iodide symporter expression. Endocrinology. 2006;147(4):2035-42. doi: 10.1210/en.2005-0805. PubMed PMID: 16339205.
45. Flader M, Kurzawa P, Maldyk J, Sygut J, Harasymczuk J, Kropinska A, Handkiewicz-Junak D, Jarzab B, Kotulska K, Niedziela M. Papillary thyroid carcinoma in a boy with familial tuberous sclerosis complex attributable to a TSC2 deletion-a case report. Curr Oncol. 2017;24(5):e423-e8. Epub 2017/11/02. doi: 10.3747/co.24.3555. PubMed PMID: 29089812; PMCID: PMC5659166.
46. Auladell M, Boronat S, Barber I, Thiele EA. Thyroid nodules on chest CT of patients with tuberous sclerosis complex. Am J Med Genet A. 2015;167A(12):2992-7. Epub 2015/09/04. doi: 10.1002/ajmg.a.37339. PubMed PMID: 26332136.
47. Dicorato P, Calvanese A, Maiuolo A, D'Alessandri M, Grani G, Ruggieri M, Fumarola A. Medullary thyroid carcinoma and tuberous sclerosis. Endocr Pathol. 2009;20(2):141-4. Epub 2009/05/09. doi: 10.1007/s12022-009-9077-z. PubMed PMID: 19424876.
48. Adhvaryu K, Shanbag P, Vaidya M. Tuberous sclerosis with hypothyroidism and precocious puberty. Indian J Pediatr. 2004;71(3):273-5. Epub 2004/04/15. doi: 10.1007/BF02724284. PubMed PMID: 15080418.
49. Bereket A, Wilson TA. Thyroid dysgenesis and the dysplasia hypothesis in tuberous sclerosis. Am J Med Genet. 1993;47(3):417-9. Epub 1993/09/01. doi: 10.1002/ajmg.1320470324. PubMed PMID: 8135291.
50. Ilgren EB, Westmoreland D. Tuberous sclerosis: unusual associations in four cases. J Clin Pathol. 1984;37(3):272-8. Epub 1984/03/01. doi: 10.1136/jcp.37.3.272. PubMed PMID: 6142060; PMCID: PMC498698.
51. Dworakowska D, Grossman AB. Are neuroendocrine tumours a feature of tuberous sclerosis? A systematic review. Endocr Relat Cancer. 2009;16(1):45-58. Epub 2008/11/04. doi: 10.1677/ERC-08-0142. PubMed PMID: 18978035.
52. Bianco AC, Anderson G, Forrest D, Galton VA, Gereben B, Kim BW, Kopp PA, Liao XH, Obregon MJ, Peeters RP, Refetoff S, Sharlin DS, Simonides WS, Weiss RE, Williams GR, American Thyroid Association Task Force on A, Strategies to Investigate Thyroid Hormone E, Action. American Thyroid Association Guide to investigating thyroid hormone economy and action in rodent and cell models. Thyroid. 2014;24(1):88-168. Epub 2013/09/05. doi: 10.1089/thy.2013.0109. PubMed PMID: 24001133; PMCID: PMC3887458.
53. Hernandez O, Way S, McKenna J, 3rd, Gambello MJ. Generation of a conditional disruption of the Tsc2 gene. Genesis. 2007;45(2):101-6. Epub 2007/01/25. doi: 10.1002/dvg.20271. PubMed PMID: 17245776.
54. Kusakabe T, Kawaguchi A, Kawaguchi R, Feigenbaum L, Kimura S. Thyrocyte-specific expression of Cre recombinase in transgenic mice. Genesis. 2004;39(3):212-6. doi: 10.1002/gene.20043. PubMed PMID: WOS:000223221500008.
55. Capen CC. Correlation of mechanistic data and histopathology in the evaluation of selected toxic endpoints of the endocrine system. Toxicol Lett. 1998;102-103:405-9. doi: 10.1016/s0378-4274(98)00244-6. PubMed PMID: 10022287.
56. Wade MG, Parent S, Finnson KW, Foster W, Younglai E, McMahon A, Cyr DG, Hughes C. Thyroid toxicity due to subchronic exposure to a complex mixture of 16 organochlorines, lead, and cadmium. Toxicol Sci. 2002;67(2):207-18. doi: 10.1093/toxsci/67.2.207. PubMed PMID: 12011480.
57. Blancquaert S, Wang L, Paternot S, Coulonval K, Dumont JE, Harris TE, Roger PP. cAMP-dependent activation of mammalian target of rapamycin (mTOR) in thyroid cells. Implication in mitogenesis and activation of CDK4. Mol Endocrinol. 2010;24(7):1453-68. Epub 2010/05/21. doi: 10.1210/me.2010-0087. PubMed PMID: 20484410; PMCID: PMC2903905.
58. Coulonval K, Bockstaele L, Paternot S, Dumont JE, Roger PP. The cyclin D3-CDK4-p27kip1 holoenzyme in thyroid epithelial cells: activation by TSH, inhibition by TGFbeta, and phosphorylations of its subunits demonstrated by two-dimensional gel electrophoresis. Exp Cell Res. 2003;291(1):135-49. Epub 2003/11/05. doi: 10.1016/s0014-4827(03)00392-6. PubMed PMID: 14597415.
59. Motti ML, Boccia A, Belletti B, Bruni P, Troncone G, Cito L, Monaco M, Chiappetta G, Baldassarre G, Palombini L, Fusco A, Viglietto G. Critical role of cyclin D3 in TSH-dependent growth of thyrocytes and in hyperproliferative diseases of the thyroid gland. Oncogene. 2003;22(48):7576-86. Epub 2003/10/25. doi: 10.1038/sj.onc.1207055. PubMed PMID: 14576819.

60. Van Keymeulen A, Bartek J, Dumont JE, Roger PP. Cyclin D3 accumulation and activity integrate and rank the comitogenic pathways of thyrotropin and insulin in thyrocytes in primary culture. Oncogene. 1999;18(51):7351-9. Epub 1999/12/22. doi: 10.1038/sj.onc.1203164. PubMed PMID: 10602491.
61. Nilsson M, Fagman H. Development of the thyroid gland. Development. 2017;144(12):2123-40. doi: 10.1242/dev.145615. PubMed PMID: 28634271.
62. Eggo MC, Bachrach LK, Burrow GN. Interaction of TSH, insulin and insulin-like growth factors in regulating thyroid growth and function. Growth Factors. 1990;2(2-3):99-109. doi: 10.3109/08977199009071497. PubMed PMID: 2160262.
63. Cass LA, Meinkoth JL. Differential effects of cyclic adenosine 3',5'-monophosphate on p70 ribosomal S6 kinase. Endocrinology. 1998;139(4):1991-8. doi: 10.1210/endo.139.4.5880. PubMed PMID: 9528986.
64. Sipos JA, Mazzaferri EL. Thyroid cancer epidemiology and prognostic variables. Clin Oncol (R Coll Radiol). 2010;22(6):395-404. Epub 20100603. doi: 10.1016/j.clon.2010.05.004. PubMed PMID: 20627675.
65. LiVolsi VA. Papillary thyroid carcinoma: an update. Mod Pathol. 2011;24 Suppl 2:S1-9. doi: 10.1038/modpathol.2010.129. PubMed PMID: 21455196.
66. Soares P, Celestino R, Melo M, Fonseca E, Sobrinho-Simoes M. Prognostic biomarkers in thyroid cancer. Virchows Arch. 2014;464(3):333-46. Epub 20140201. doi: 10.1007/s00428-013-1521-2. PubMed PMID: 24487783.
67. Tavares C, Coelho MJ, Melo M, da Rocha AG, Pestana A, Batista R, Salgado C, Eloy C, Ferreira L, Rios E, Sobrinho-Simoes M, Soares P. pmTOR is a marker of aggressiveness in papillary thyroid carcinomas. Surgery. 2016;160(6):1582-90. Epub 2016/08/31. doi: 10.1016/j.surg.2016.06.050. PubMed PMID: 27574774.